REMOTE SENSING OF AURORAL PLASMAS

P. Zarka*

Abstract

In this paper we review the recent results of several methods for deriving informations about the plasma environments of the five 'Radio–Planets' (The Earth, Jupiter, Saturn, Uranus and Neptune) from remote observations of their auroral radio emissions. This becomes possible due to the increasingly better quantitative understanding of their most probable generation mechanism – the Cyclotron Maser Instability –, and also of the near–source wave propagation and polarization transfer. Constraints on total electron densities and on the energy of hot electrons in the radio source regions are obtained.

1 Introduction

Auroral radio emissions involve negligible energies by magnetospheric standards, and are also a 'downstream' phenomenon in the sense that they are the final product of chain of processes including large scale magnetospheric dynamics, particle acceleration, and the microscopic generation mechanism itself. For these reasons, they are often considered as a magnetospheric phenomenon of minor importance. However, these radio emissions (and also UV and IR auroral emissions) carry the only information available remotely about the key high–latitude regions of planetary magnetospheres from which they originate. As their generation mechanism depends crucially on the magnetic field topology and on the electron densities and energies in the source regions, its present good understanding makes auroral radio emissions modeling a very powerful tool for probing remotely these high–latitude magnetospheric regions.

The methodology is actually that of spectroscopy, applied to the planetary auroral emissions: Instead of interpreting emission or absorption line spectra generated by bound electrons with the help of laboratory measurements for determining constituents abundances and temperatures, one interprets here the continuum emission of unbound energetic electrons with the help of a theory – the Cyclotron Maser Instability (CMI) – developed mainly to explain the Terrestrial Kilometric Radiation (TKR) generation, for deriving the total electron densities, the hot electrons energies, and their variations in the radio source regions.

* *Observatoire de Paris, Section de Meudon, 92195 Meudon Cedex, France*

Although relying upon an old idea, the use of this remote sensing technique is very new in the field of planetary radio emissions (nearly all the results reported here are posterior to the 2^{nd} Planetary Radio Emissions conference). Detailed scenarii for radio waves generation through the CMI have indeed been elaborated recently, after in–depth comparative studies of the extensive observations available mainly for the radio emissions of the Earth, Jupiter and Saturn over broad frequency ranges and with good spectral and temporal resolutions, and also with the input from in–situ measurements of particle populations and plasma waves in the Earth's auroral regions.

After recalling the limitations and advantages of radio observations, I will present a brief overview of the present state of our observational and theoretical knowledge of the auroral radio emissions and their generation. This provides the frame for the following sections which deal with the remote sensing of the density in the Earth's auroral plasma cavities, and with that of the distribution of Saturn's auroral plasma and the characteristic energy of its hot component. The possible existence of plasma cavities at Jupiter, Uranus and Neptune is briefly discussed in the last sections.

2 The radio observations: Limitations and advantage

Observational limitations include the very poor angular resolution which affects the observations at decameter to kilometer wavelengths ($\lambda/D \geq 1$!, λ being the wavelength and D the characteristic size of the antenna) and prevents any direct determination of the radio source locations, and the different amount and geometrical coverage of the radio observations available for the five radio planets: The TKR has been observed by many satellites from any possible viewing geometry; the Jovian decameter (DAM) emission has been observed for years from ground–based radiotelescopes (as the Nançay decameter array, in France), and also for a few months by the Voyager 1 & 2 Planetary Radio Astronomy (PRA) experiments, mainly from near–equatorial Jovicentric latitudes; all the other low–frequency radio emissions (the hectometer – HOM – and kilometer – KOM – radiations from Jupiter, and Saturnian, Uranian and Neptunian kilometric radiations – SKR, UKR & NKR) have been discovered and exclusively observed by Voyager–PRA (except for a few HOM observations by the RAE1 and IMP6 satellites), from only a few directions of observation, and over periods from only one month (UKR, NKR) to more than one year (HOM, SKR) [Genova, 1987; Zarka, 1992]. At Uranus and Neptune, the available radio data sets are very limited, and our knowledge of the magnetospheric environment (particle populations, magnetic field topology, radio sources locations) of these planets is very poor and provides little context for any detailed study [Boischot, 1988].

However, as auroral radio emissions are thought to be generated along high–latitude magnetic field lines, close to the local gyrofrequency, the lack of direct angular resolution is somewhat balanced by the broad frequency range ($\Delta f \sim f_{observed}$) and the good spectral resolution ($\delta f/f \sim 10^{-1} - 10^{-2}$) of the observations, which provide an effective spatial resolution of 0.01 to 0.1 planetary radius along the source magnetic field lines extending over several planetary radii, assuming that those are identified. Also, the good temporal resolution of radio observations (a few seconds for PRA; down to 10 ms for ground–based observations) and the extensive and continuous data sets available (at least for

TKR, DAM, HOM and SKR) allow for a statistical approach and the monitoring of the phenomena studied.

It is useful to summarize here the characteristics of the Voyager–PRA experiments [Warwick et al., 1977], whose data are the main input for the following studies: The PRA receiver, connected to two 10–m orthogonal monopole antennas, sweeps in 6s through 198 channels grouped in two linear bands, measuring flux densities in each channel alternately in left–hand (LH) and right–hand (RH) circular polarization. The number of channels, channel bandwidth and (linear) frequency spacing are respectively 70, 1 kHz and 19.2 kHz in the low–frequency band (from 1.2 to 1326.0 kHz, where TKR, HOM, SKR, UKR and NKR were observed), and 128, 200 kHz and 307.2 kHz in the high–frequency band (from 1.2 to 40.2 MHz, range of the Jovian DAM emission).

3 Overview of the auroral planetary radio emissions

3.1 Observational properties of auroral radio emissions

The observational properties of auroral radio emissions at the time of this review can be summarized as follows [Zarka, 1992] :

- Their very high brightness temperature ($T_B > 10^{14-15} K$) implies that they are nonthermal coherent emissions. The average emitted power ranges between 10^7 Watts (UKR, NKR) and 10^{11} Watts (DAM), and represents typically a fraction $\sim 10^{-5}$ of the incident solar wind power, but the radio emissions are generated within very limited boundary regions of the magnetospheres.

- They are emitted from sources along high magnetic latitude field lines, extending over several planetary radii. Emission is thought to occur mainly in the R–X mode, close to the local gyrofrequency (f_c), or more exactly close to the X mode cutoff frequency
$$f_X = f_c/2 + (f_p^2 + f_c^2/2)^{1/2}\,, \tag{3.1}$$
where f_p is the electron plasma frequency. The plasma density is extremely low in the source regions ($f_p/f_c < 0.3$), so that $f_X \sim f_c(1 + (f_p/f_c)^2)$.

- The instantaneous emission beam can be represented as a hollow, widely open cone [Zarka, 1988]. Its source either rotates with the planetary magnetic field (case of Jovian emissions and of the 'Smooth' components of UKR and NKR), or is fixed in local time (LT) and turned successively on and off with the planetary rotation (case of TKR, SKR, and possibly of the 'Bursty' components of UKR and NKR).

- The emissions are 100% circularly polarized (with the exception of DAM and maybe part of NKR – see below) [Lecacheux, 1988].

- 'Smooth' and 'Bursty' radio components are observed at nearly all the radio planets; the former vary with timescales of minutes to hours, while the latter exhibit fluctuations as fast as a few milliseconds, together with very narrowbanded structures in their dynamic spectra (down to 10 Hz for the TKR [Baumback and Calvert, 1987]).

- Finally, the auroral radio emission activity is correlated with the UV one and, as observed at the Earth, with precipitating electrons (with 'inverted–V' spectra) or more generally with the presence of unstable electron populations in the source regions (showing loss–cone, 'bumps' of quasi–trapped particles, or 'holes' with keV energy in their distribution function [Mizera and Fennell, 1977]).

3.2 The Viking source model

The Swedish satellite Viking (launched Feb. 1986) provided a much more comprehensive view of the TKR source regions, based on the wave and particle observations it performed during its many source crossings [de Feraudy et al., 1987, 1988; Bahnsen et al., 1989; Louarn et al., 1990; Hilgers et al., 1991; Hilgers, this book]. The most significant discoveries included the following facts :

- The emitted frequency is equal or below the local gyrofrequency in the source regions.
- Individual source regions are only a few kilometers across, and hot plasma dominated (a few keV). The electron distribution corresponds to a 'quasi–trapped' population inside the sources, and to enhanced loss–cones on the edges of the sources.
- Electron and ion beams were also observed in or at the edges of the sources.

The emerging picture is that of filamentary and hot plasma dominated TKR sources located in small–scale acceleration regions, by comparison with the old picture of a large scale plasma cavity located below an acceleration region, depleted but still cold plasma dominated.

3.3 The present state of the theory

The present state–of–the–art of the theory for auroral radio emissions generation is centered about the CMI, first proposed for explaining the TKR generation [Wu and Lee, 1979], and which has gained the status of 'best–candidate mechanism' due to its consistency with the observations at all the radio–planets, as summarized above (including the Viking observations at the Earth). The reader is refered to the extensive reviews by Wu [1985] and Le Quéau [1988] of the CMI, as we will recall here only a few points of importance.

The CMI is a resonant interaction between an unstable electron population and electromagnetic (mainly X mode) waves, leading to the wave amplification through direct conversion of the electrons free energy into electromagnetic energy. It has thus the high efficiency required by the observations. In its first formulation [Wu and Lee, 1979], only growth rates were computed from loss–cone distributions in the frame of a homogeneous, cold–plasma dominated source model. Le Quéau et al. [1985] and Zarka et al. [1986] extended this study to inhomogeneous source models (taking into account the magnetic

field gradient, as it is necessary for all emissions but the DAM), considered other unstable populations ('holelike') and calculated the emitted flux, consistent with the observed TKR fluxes (recently re–evaluated by one order of magnitude after re–analysis of ISEE radio data [Benson and Fainberg, 1991]). Following Viking results, Le Quéau and Louarn [1989] and Louarn et al. [1990] developed a hot plasma dominated source model, showing that the X mode cutoff is then expected to decrease – eventually below f_c – as it was observed, and that quasi–trapped electrons become then a very efficient free energy source for driving the CMI (which turns from a convective to a quasi–absolute instability), leading to increased fluxes. With such an efficient amplification mechanism, it was relevant to examine the possible saturation processes [Le Quéau et al., 1984; Pritchett, 1984], and the most relevant one in the case of emissions instantaneously very narrowbanded ($\delta f/f \leq 10^{-2}$) seems to be the nonlinear trapping of the electrons in the wave electric field [Le Quéau, 1988]. Expecting that the Saturnian magneto–plasma is simple to model (quasi axial planetary magnetic field and very low plasma density in the high–latitude regions due to the planet's rapid rotation, suggesting that small–scale plasma cavities may be absent) Galopeau et al. [1989] computed a trapping–saturated spectrum for the SKR emission, which was found in very good agreement with the observations (see below). Finally, the extremely high intensity and sporadic and narrowband nature of the 'bursty' planetary radio components led Calvert [1982, 1988] to suggest the possible occurrence of a 'Lasing' process between the plasma density walls of the auroral cavities, leading to mode selection and enhanced gains.

The above overview intends to show the high degree of refinement reached by the modeling of planetary radio emissions through the CMI, which may now be used to derive, from remote radio observations, information on the auroral plasma (and magnetic field) where these emissions originate.

4 The Earth's Auroral Plasma Cavity after Viking measurements: From singular to plural

On the basis of ISIS–1 [Benson and Calvert, 1979] and Hawkeye first in–situ measurements in TKR source regions, Calvert [1981] proposed the concept of a large–scale plasma cavity at high latitudes ($70° \pm 3°$ magnetic latitude), between ~ 1.5 and 3 R_E geocentric distance, with electron densities as low as 1 cm^{-3}. S3–3 satellite measurements at about 2 R_E [Temerin et al., 1981; Temerin, 1984], and DE–1 measurements up to 4.7 R_E [Persoon et al., 1988] confirmed these low plasma densities at auroral latitudes, and showed evidence for their association with acceleration processes (field–aligned ion beams, up–flowing ions, electrostatic shocks) occurring within auroral structures with $\sim 1°$ invariant latitude width. Finally, Viking measurements inside TKR source regions have shown that these coincide with small–scale ($< 1°$ latitude) acceleration structures and plasma density depletions [Bahnsen et al., 1989; Louarn et al., 1990; Perrault et al., 1990; Hilgers et al., 1991].

Hilgers [1992 and this book] performed an exhaustive study of the Earth's auroral plasma cavities from Viking Langmuir probe measurements between 1.5 and 3 R_E geocentric

distance, and showed that the concept of Calvert's large–scale plasma cavity should be abandoned to the profit of that of filamentary, small–scale depletions with densities of a few electrons per cm^3, immersed in a medium ~ 10 times denser. TKR was found to be emitted only in those most tenuous depletions, where $f_p/f_c \leq 0.14$ (a value consistent with the constraints fixed by the hot plasma CMI theory with a few keV electrons).

As a consequence, TKR observation can be potentially considered as a remote diagnosis of the plasma density in its instantaneous source region. The difficulty is to locate precisely this source at the time of the observation. Knowing that TKR is generated very close to f_c, along field lines often connected with UV bright spots or discrete arcs in the auroral oval, this can be done quite reliably through UV imaging [Huff et al., 1988] and/or determination of the direction of incoming radio waves (as successfully attempted with DE–1 rotating electric dipole antenna [Calvert, 1985]).

5 Remote sensing of Saturn's high–latitude plasma from SKR modelling

Our knowledge of SKR comes exclusively from Voyager 1 & 2 PRA observations (see the review of Kaiser et al. [1984]). As its spectrum is in the range $\sim 1 - 1230$ kHz, it was observed only in the PRA low–frequency band. SKR has been interpreted as X mode emission from high–latitude ($70° - 80°$) northern and southern sources, very similar to the auroral nonthermal emissions from the other radio–planets. Its sources are fixed relative to the Sun direction and close to noon (local time) [Kaiser and Desch, 1982; Lecacheux and Genova, 1983]. The SKR spectral peak lies between 100 and 400 kHz, with a flux density about 10^{-19} $Wm^{-2}Hz^{-1}$ when normalized to 1 AU. The observed spectra present generally a slow decrease towards low frequencies (below 100 kHz) and a steeper one at high frequencies (above ~ 600 kHz).

Using a simple description of Saturn's auroral magnetoplasma, Galopeau et al. [1989] derived a theoretical model of the SKR spectrum in good agreement with the observed one. The assumptions they used (and that we will keep on using in the parametric study below) can be summarized as follows :

- The northern and southern SKR sources were considered to be located along L=15 field lines (footprint at 75° latitude); this is a simplifying assumption, as recent studies (see Galopeau, this book) have shown that the SKR sources appear indeed fixed in local time, but possibly distributed along high–latitude North and South 'croissants' extending from $\sim$ 0900 LT to $\sim$ 1900 LT; the main or most probable source location is about noon LT, but at latitudes higher than 75°; however, the computed SKR spectrum does not depent crucially on the precise source location.

- The planetary magnetic field was taken as quasi–dipolar in the source region. Again this is a good approximation of the Saturn's Z3 model magnetic field [Connerney et al., 1984], or of its modified expression including a high–latitude magnetic anomaly, as derived by Galopeau et al. [1991] from the statistical variations of the rotation–modulated SKR high–frequency limit. The deviation of the dipolar field from these

more realistic models only slightly affects the high–frequency part of the SKR spectrum.

- The (cold) plasma density around Saturn was modelled, as constrained by Voyager 1 and 2 measurements [Tyler et al., 1982; Bridge et al., 1982; Lazarus and McNutt, 1983], as the sum of the contributions from the ionosphere and from an equatorial plasma disc

$$N_e = N_e(ionosphere) + N_e(disc) = N_i^p e^{-(r-R_p)/H_i} + N_d^o L^{-3} e^{-(z/H_d)^2}\,, \qquad (5.1)$$

where N_i^p is the ionospheric peak electron density – Voyager 1 ingress occultation profile at 73° Southern latitude gave $N_i^p = 2.4 \times 10^4$ cm^{-3} at an altitude $\sim$ 2400 km above the 1–bar level [Atreya et al., 1984] –, R_p is the planetary radius at the ionospheric peak, r is the Kronocentric distance, $N_d^o = 2400$ cm$^{-3} R_S^3$, R_S is the equator radius of Saturn (60330 km), L is the magnetic shell parameter, z is the elevation above the equatorial plane, and H_i and H_d are the characteristic scale heights of the ionosphere and the plasma disc. Voyager measurements (plasma experiment and radio occultations) gave the following ranges for H_i and H_d:

$$0.01 R_S \leq H_i \leq 0.02 R_S\,, \qquad \text{and} \qquad 0.5 R_S \leq H_d \leq 1.0 R_S\,. \qquad (5.2)$$

These numbers should not be considered as absolutely tight constraints for the auroral regions, as the in–situ plasma measurements were performed along Voyager trajectories, i.e. mainly in near–equatorial regions. It is important to note that this plasma density model leads to very low f_p/f_c (< 0.1) ratios in the SKR source regions, low enough for the CMI to operate without explicit need for an auroral plasma cavity.

- Finally, as the detailed distribution function of energetic auroral electrons is not known for any planet other than the Earth, a maximum–saturated SKR spectrum was calculated. As explained above, nonlinear trapping was considered as the most relevant process for estimating the saturation electric field in the source region. The spectral intensity was then deduced from the self–consistent optimization of CMI (in the frame of a cold plasma dominated source model): The vertical size of the source at each frequency is limited by the magnetic field variations, and the minimum perpendicular size for the CMI to be fully efficient is the cross–section of a magnetic flux tube with a $\sim 0.5°$ footprint diameter, which is a reasonable size for instantaneous auroral electron precipitation region [Galopeau et al., 1989]. With this hypothesis of saturation, only the characteristic energy of hot electrons in the direction perpendicular to the local magnetic field ($E_\perp$) is needed for computing the SKR maximum spectrum. From Voyager UV measurements, Sandel et al. [1982] showed that the parallel energy of the precipitating electrons responsible for the Saturnian auroral glow (which is localized on the border of the polar cusp, as the SKR sources probably are) is of the order of 10 keV. $E_\perp$ was taken $\sim$ 1 keV by Galopeau et al. [1989].

The only free parameters in the above model are $E_\perp$ and the plasma scale heights H_i and H_d. For given values of these 3 parameters, the SKR spectrum is completely defined, in

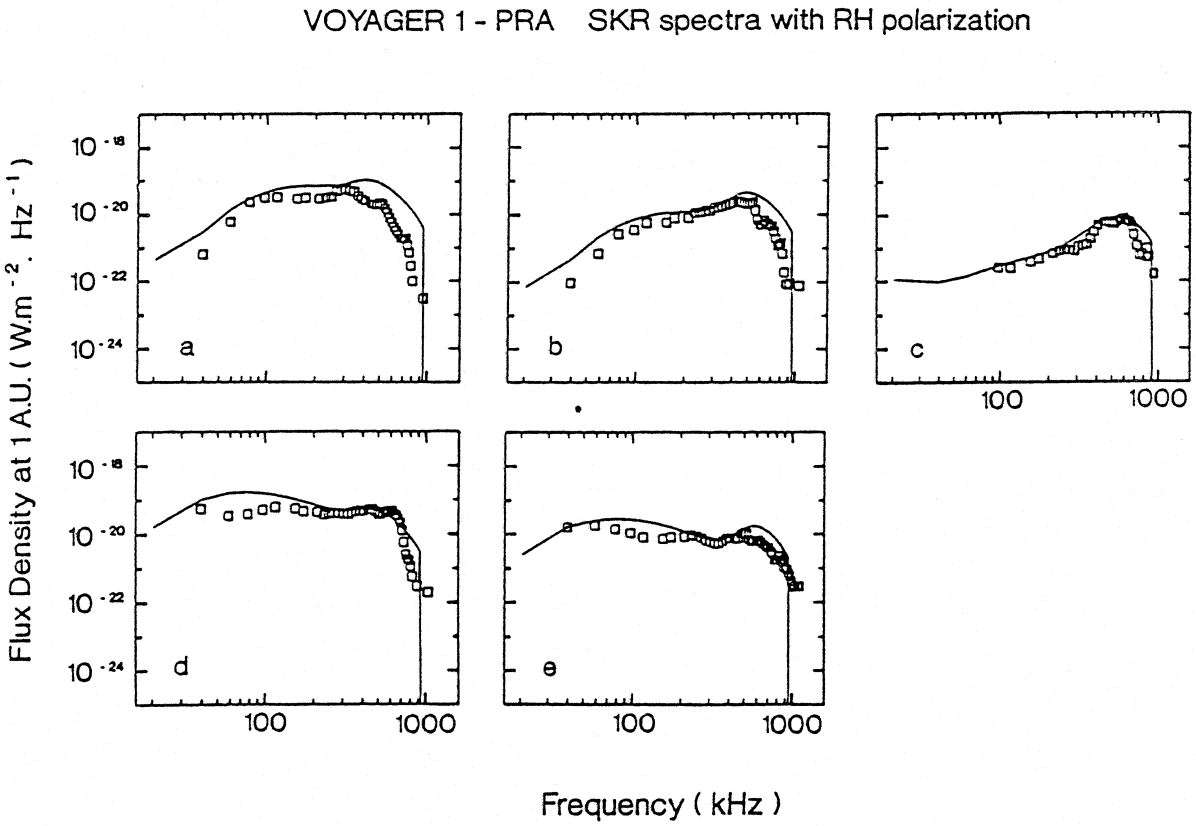

Figure 1: Best fit of the computed SKR spectra (continuous lines) to those observed by the Voyager–PRA experiment (squares) allows to derive the profile of total electron density and the characteristic energy of hot electrons in the source region. Table 1 lists the parameters of observation and the inferred plasma parameters for the five spectra displayed on this Figure. The displayed data correspond to the Voyager 1 post–encounter trajectory. The fit is of the least–squares type, weighted by the observed spectral intensity and for compensating the linear sampling of the PRA low–frequency band.

flux density as well as in shape and frequency extent. As the observed SKR spectrum is known to vary much, not only with the direction of observation (from before to after Voyager closest approaches to Saturn [Kaiser et al., 1981]), but also with the planetary rotation [Genova et al., 1983], it was interesting to check, through a parametric study of the SKR theoretical spectrum, if these variations can be explained through variations of H_i, H_d and $E_\perp$.

Figure 1 shows SKR peak spectra observed at five different times – listed in Table 1 – shortly after Voyager 1 closest approach to Saturn, with a high signal to noise ratio. Only the dominant emission at that time, i.e. RH polarized and coming from the northern source, was considered, and the peak SKR intensity detected during a 53 min. interval centered on the times of Table 1 (corresponding to $1/12^{th}$ of the planetary rotation) is plotted versus frequency. As the SKR sources are fixed in local time, the Sun's longitude is the relevant parameter for characterizing the emission occurrence as a function of the planetary rotation, and is also given in Table 1. On Figure 1, the best fit theoretical spectra are superimposed to the observed ones. The agreement is excellent, and the

Table 1: Center time (in Day of Year 1980, SpaceCraft Event Time) and Sub–Solar longitude (Sol–SLS) of the five observed spectra of Figure 1, together with the inferred ionospheric and disc scale heights (H_i and H_d) describing the total electron density profile in the SKR source region, and the characteristic perpendicular energy ($E_\perp$) of the hot electrons involved in the generation of the corresponding spectra.

DOY 1980	SCET (hhmm)	Sol–SLS (°)	H_i (R_S)	H_d (R_S)	$E_\perp$ (keV)	
320	2129	165	0.014	0.7	1	(a)
321	1608	75	0.014	0.7	2	(b)
323	0901	15	0.016	0.7	8	(c)
325	1510	45	0.015	0.9	2	(d)
325	1937	195	0.014	0.9	4	(e)

corresponding values of H_d, H_i and $E_\perp$ are also listed in Table 1.

This work, done systematically for consecutive spectra, computed each over 30° sub–solar longitude intervals (in RH polarization, i.e. for northern SKR emission), for a period of 3 months ($\sim$ 200 planetary rotations) of observations around Voyager 1 closest approach to Saturn, led to $< H_d >= 0.8 \pm 0.1 R_S$ and $1 \leq E_\perp \leq 4$ keV. The scale height H_i, which affects the higher frequency part of the spectrum, is less tightly constrained but generally found within the range 0.01 – 0.02 R_S, consistent with Voyager observations [Zarka and Galopeau, to be submitted, 1992]. The corresponding vertical profile of the electron density in Saturn's auroral region (Equation (5.1) with R_p = 1.04 R_S and H_i = 0.015 R_S) is plotted on Figure 2b. Isodensity contours are schematically sketched in Figure 2a in the high–latitude regions where Equation (5.1) is expected to describe satisfactorily the plasma density variations, together with those derived from the Voyager plasma measurements in the vicinity of the equatorial plane [Richardson and Sittler, 1990] to which they are complementary and might reconnect.

From the above study, no systematic dependence of the electron density profile in the SKR source region was found with respect to the planetary rotation, as was expected from the fact that the source is fixed in latitude and local time. But the perpendicular energy of the hot electrons responsible for the emission seems to be modulated by the planetary rotation in the range 1–5 keV. This modulation could depend on a magnetic field anomaly governing the electron precipitations (maximum $E_\perp$ is observed for maximum negative gradient of the magnetic field predicted by the model of Galopeau et al. [1991]).

A few additional remarks can be done about the assumptions underlying the above results :

- The saturation hypothesis is supported by the fact that we compared the theoretical spectra with peak observed SKR spectra, which represent the most intense planetary radio emission in the range 100–400 kHz (see Fig. 3 of [Zarka, 1992]).
- The assumption of a cold plasma dominated source is questionable, in the light of recent Viking observations (see above), but it has much less influence on the

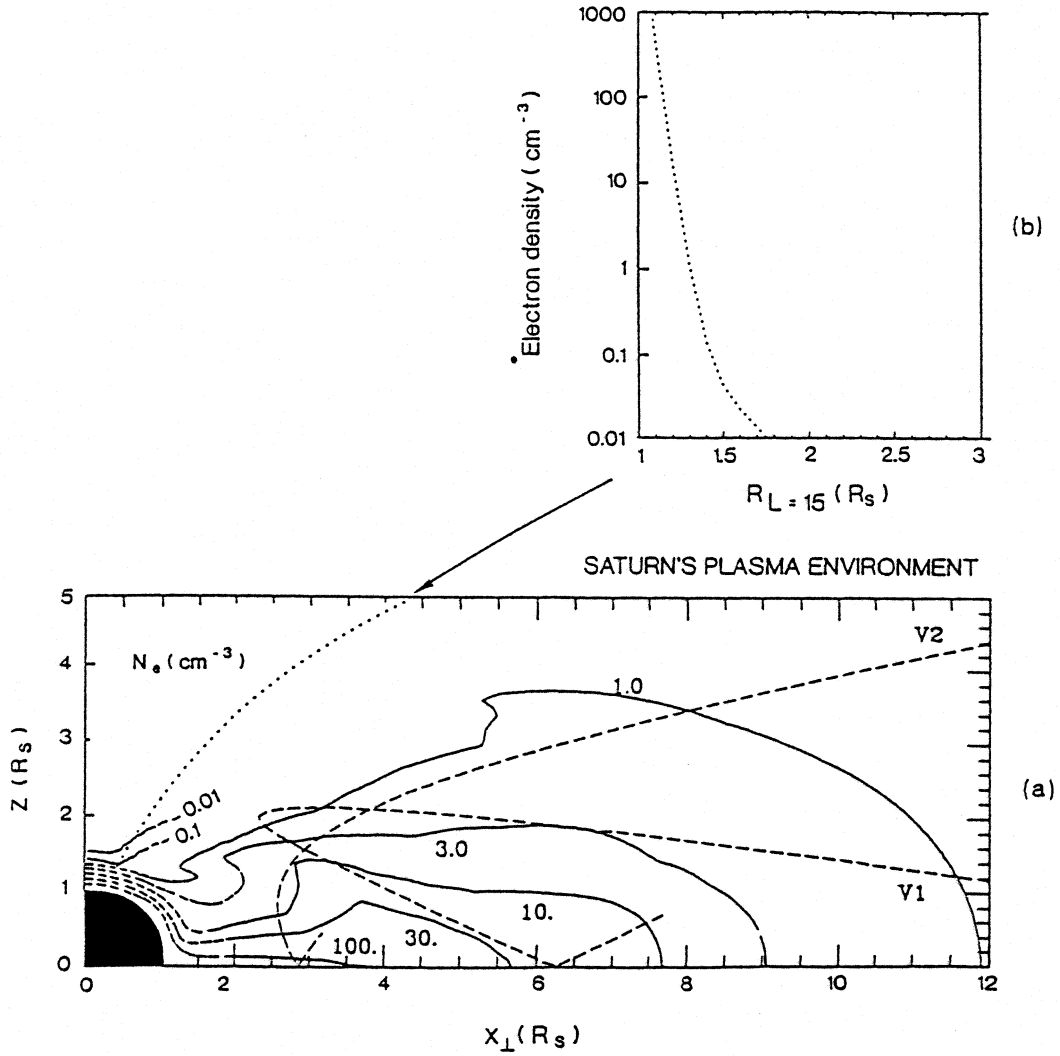

Figure 2: (a) Sketch of the isocontours of the remotely–sensed electron density above Saturn's northern auroral region, together with that directly measured in lower latitude regions by the Voyager plasma experiment (adapted from [Richardson and Sittler, 1990]). (b) Corresponding profile of the total electron density in the SKR source region (with $H_d = 0.8\ R_S$, $R_p = 1.04\ R_S$ and $H_i = 0.015\ R_S$), along the $L = 15$ field line (dotted line of (a)).

saturated flux, as can be deduced from [Galopeau et al., 1989], than on the linear wave growth.

- Finally, the perpendicular source size could be considered as an additional free parameter for fine–tuning the overall level of the saturated spectrum, although the value of 0.5° invariant latitude seems adequate.

The values of H_i, H_d and $E_\perp$ deduced from the systematic fit of the theoretical and observed SKR spectra also show long–term variations, presently investigated, and probably linked to an external (solar wind) influence on Saturn's auroral plasma.

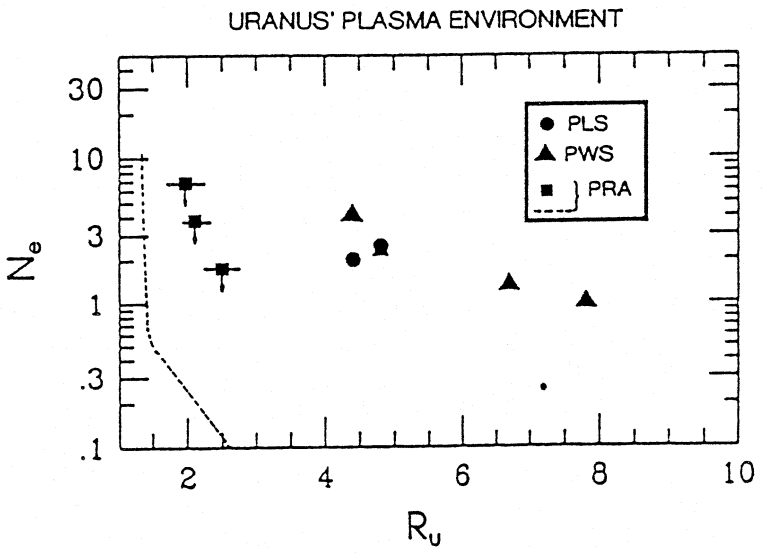

Figure 3: Comparison of the electron density variations in the vicinity of Uranus deduced (i) from Voyager in–situ plasma science (PLS experiment – o) and plasma waves (PWS experiment – Δ) measurements, and remote radio observations (PRA experiment – squares) at low magnetic latitudes, and (ii) from PRA observations only at high magnetic latitudes (L ∼ 33 – dashed line). Adapted from [Kaiser et al., 1989] and [Carr and Gulkis, 1988].

6 Electron densities near Uranus and Neptune from Voyager–PRA observations: Existence of small–scale auroral cavities ?

The same concepts as above were applied in a more rudimentary way to the more limited observations of Uranus radio emissions to derive some constraints on the electron density in the vicinity of the magnetic equator and of the magnetic poles. Among the zoo of Uranian radio emissions (up to 7 separate components [Desch, 1991]), the so–called Narrowband–Smooth one, observed at about 60 kHz, was successfully interpreted by Kaiser et al. [1989] as R–X mode emission originating from a distributed source surrounding Uranus at the magnetic equator, at a radial distance of 2 to 3 planetary radii. Due to the peculiar geometry of Uranus magnetic field (equivalent dipole tilted by 58.6° from the rotation axis [Ness, 1988]), preventing the accumulation of plasma in the equatorial regions, the CMI still appears as a viable mechanism for generating this equatorial emission. The constraint put on the ratio f_p/f_c by X mode emission through the CMI (typically $f_p/f_c < 0.3$ [Melrose et al., 1984; Le Quéau et al., 1985]) allowed Kaiser et al. [1989] to infer upper limits on the equatorial electron density near Uranus. They are displayed on Figure 3 (squares), together with the electron densities directly measured by the plasma science [McNutt et al., 1987] and plasma waves [Kurth et al., 1987] experiments onboard Voyager.

On the other hand, the Broadband–Smooth component [Desch et al., 1991], observed between 100 and 850 kHz, has been interpreted as 'usual' R–X mode emission from the auroral, high–latitude regions of the magnetosphere of Uranus. Again, the CMI requirements allowed Carr and Gulkis [1988] to put constraints on the total electron density along the supposedly $L = 33$ source field line (dashed line of Figure 3). The constraints summarized on Figure 3 are very crude upper limits, which depend on the source location of the Broadband-Smooth component. The $L = 33$ source location was deduced by Carr and Gulkis [1988] from a model of the emission beaming. However, 6 other independent attempts for locating the source of the Broadband-Smooth component

through various methods yielded as many significantly different source locations, spread over $\sim 30°$ in latitude and longitude around Uranus southern magnetic pole [Zarka and Lecacheux, 1987; Desch et al., 1991]. This large uncertainty on the source location is mainly due to the limited PRA data set available at Uranus, and to the use of the (too) simple OTD (Offset Tilted Dipole [Ness et al., 1986]) Uranian magnetic field model.

However, on Figure 3, the decrease of electron density with radial distance appears much steeper in the high–latitude region compared to the near–equatorial one. This suggests the possible existence of at least one southern auroral plasma cavity at Uranus. This existence is supported at Uranus, as well as at Neptune, by the interpretation of some observed characteristics of the intense radio bursts observed at these planets [Desch et al., 1991; Warwick et al., 1989]. From the analysis of PRA data, Farrell et al. [1991] deduced that these bursty emissions are generally beamed at two frequency–dependent angles relative to the local magnetic field in their high–latitude source. This 'double-beaming' can be explained in the frame of the CMI if the source medium is extremely depleted: Resonance between energetic electrons and electromagnetic waves may then occur for two different values of the R–X mode refractive index, or equivalently for two different angles of propagation at infinity. The deduced auroral plasma cavities are located about a few tenths of a planetary radius above the planetary surface, along $L = 28$ (Neptune) or $L = 64$ (Uranus) field lines, with electron densities as low as $0.01 - 0.1$ cm^{-3}. Again, one weak point of this remote sensing study is the determination of the radio source locations, which is indirect and quite uncertain.

7 Auroral Plasma Cavities at Jupiter and Neptune from polarization measurements ?

Constraints on the plasma density in the vicinity of auroral radio sources were recently derived in a very different way from above: While most planetary radio emissions are approx. 100% circularly polarized [Lecacheux, 1988], quantitative polarization measurements of the Jovian DAM emission performed with the Nançay spectropolarimeter [Lecacheux et al., 1991] clearly showed that this emission is elliptically polarized, with a very significant degree of linear polarization ($\sim 45\%$ to 72%). As propagation of elliptically polarized radio waves in a plasma with slowly decreasing density should lead to very rapid circularization of the observed polarization [Lecacheux, 1988; Melrose and Dulk, 1991], Lecacheux et al. [1991] interpreted the DAM persisting elliptical polarization to be most likely the original polarization produced through the CMI and retained unchanged because of extremely low plasma density in the DAM source region. The polarization produced through the CMI at large angle with respect to the source magnetic field is indeed expected to be very linear [Melrose and Dulk, 1991], and for this polarization to be retained, the characteristic frequencies in the source region should correspond to the strong mode coupling regime, in which the energy is exchanged between the characteristic modes of the medium while the wave polarization remains unchanged. This is the case if propagation occurs in a near–vacuum, with $f_p/f_c \leq 10^{-3}$ [Lecacheux, 1988]. This condition is much more drastic than that allowing simply for the CMI to operate efficiently independently of the polarization ($f_p/f_c < 0.3$).

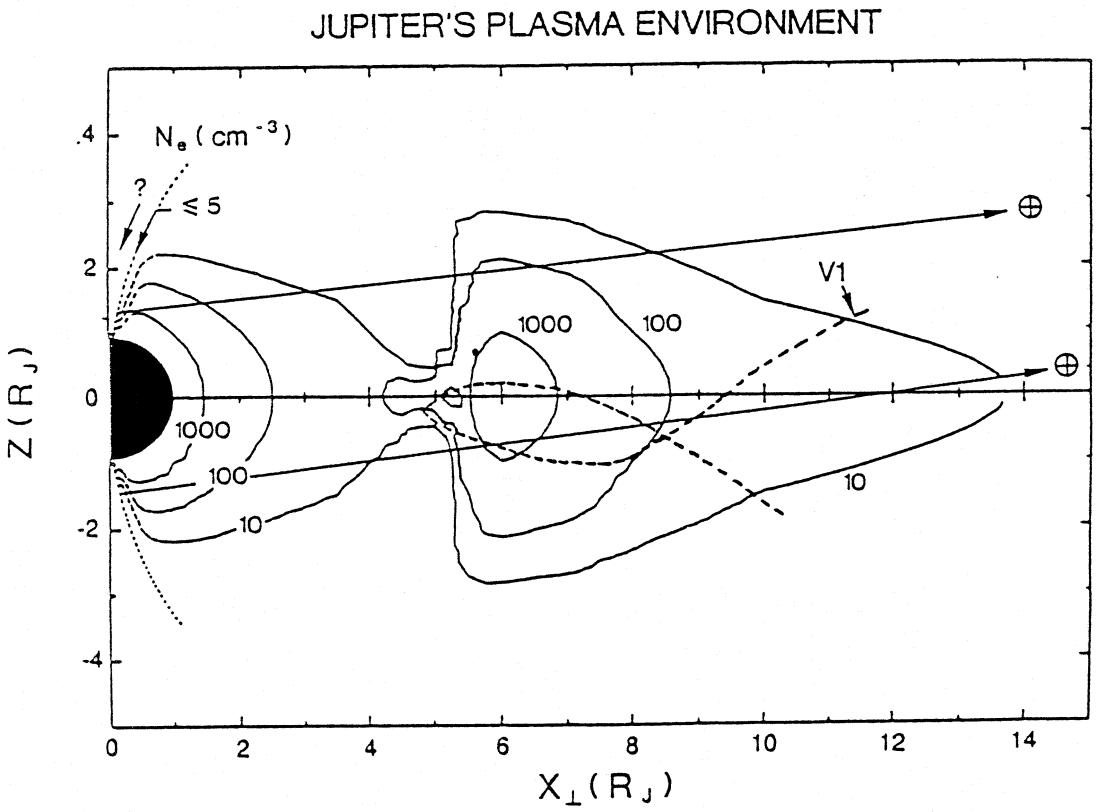

Figure 4: Isocontours of the electron density in Jupiter's vicinity from the model by Divine and Garrett [1983], together with a sketch of the auroral plasma cavity suggested by DAM polarization measurements. Typical (18 MHz) ray paths from the northern and southern auroral zones to a ground–based observer cross the Io torus (adapted from [Dulk et al., 1992]).

For decameter wavelengths, this condition implies an electron density below 5 cm^{-3} at the 30 MHz DAM source, somewhere in Jupiter's low magnetosphere, possibly along the Io flux tube and its vicinity. This density is two orders of magnitude lower than that deduced from the Divine and Garrett [1983] model. This model, built from Voyager and Pioneer near–equatorial plasma measurements, has no pretention for reliability at high latitudes and within 2–3 Jovian radii radial distance. Figure 4 is a schematic sketch illustrating the modifications that the above discussion should bring to the Divine and Garrett model. Actually, the very existence of the dense plasma region appearing on Figure 4 between ~ 1 and 4 Jovian radii (i.e. except for the ionosphere, Io's torus, and maybe a near–equatorial disc) is questionable.

Furthermore, the linearly polarized component of DAM emission propagating through the Io plasma torus is affected by Faraday rotation, and this effect was also shown to be a possible tool for probing the torus (column) density [Dulk et al., 1992].

Just before Voyager 2 closest approach to Neptune, on August 25, 1989, radio emission observed in PRA LH and RH polarization channels between $\sim$ 200 and 500 kHz was

simultaneously occulted by the planet (or rather by $f = f_X$ cutoff surfaces) [Sawyer et al., 1990; Pedersen et al., 1992]. One possible interpretation (among several others) is that the Neptunian radio component observed at that time was actually elliptically polarized (which would explain that it was detected both in LH and RH circular polarizations). In that case, the same arguments as for the Jovian case above would lead to an upper limit of about 0.03 cm^{-3} for the electron density in the corresponding source region.

8 Electron beams energy at Jupiter from S–burst properties?

For completeness, we wish to add to the above panorama of remote sensing studies the possible constraint that may be put on the energy of the precipitating electrons responsible for the so–called Jovian S–burst emission. The characteristic property of S–bursts relevant to this paper is their instantaneously narrow bandwidth ($\leq$ 100 kHz) rapidly drifting from high to low frequencies, with a drift rate df/dt as high as -10 to -20 MHz s^{-1}. No satisfactory theory exists at present time for explaining this emission. Several mechanisms have been however proposed in the literature for accounting for the observed drift rates, among which: Emission at f_c from electron beams accelerated upwards from just above the ionosphere [Leblanc et al., 1980]; conversion of electrostatic upper hybrid waves with frequency dependent group velocity into electromagnetic waves [Zaitsev et al., 1986]; 'Lasing' in a variable–size cavity [Calvert, 1988]. The first one is the most commonly referred to, and the instantaneously narrowband nature of the emission suggests that the corresponding electron beams should be very monoenergetic, with a characteristic energy of a few keV. The fact that S–burst emission occurs generally as groups or 'trains' of consecutive bursts also suggests that these upward–going electron beams should be 'pulsed' by some acceleration mechanism in or above Jupiter's upper ionosphere.

Much additional work on the subject is nevertheless necessary for obtaining the consistent generation mechanism which would be a solid basis for remote sensing studies.

9 Conclusion

The above remote sensing studies are of course preliminary, but very promising. They depend crucially on the reliability of the available theoretical models and scenarii for planetary radio emissions generation. These become quite sophisticated for accounting for the observed flux and spectra, however the theoretical modeling of the radio emissions polarization, as well as that of bursty components, are still very insufficient.

Ground–based observations (of Jovian DAM) reveal to be extremely helpful in that context, as they provide both complete polarization measurement capabilities (with the Nançay spectropolarimeter) and the possibility of performing high time and frequency resolution observations – especially of S–bursts, with the Acousto–Optical spectrograph also connected to the decameter array in Nançay.

A better knowledge of the precise radio source locations is also needed. The radio experiment onboard the Ulysses spacecraft which encountered Jupiter on February 8, 1992,

has full direction finding and polarization measurement capabilities, and should bring an invaluable contribution to the localization and polarization of Jupiter's low–frequency radio sources [Stone et al., 1992]. Ulysses will also provide new in–situ measurements of the plasma density distribution in the Io torus.

More generally, future spacecraft observations (hopefully from Galileo near Jupiter and from Cassini at Saturn) will help us to confirm the assumptions underlying our interpretation of radio observations, and will thus increase the reliability of the remote sensing techniques.

Acknowledgements: I would like to thank here J. Vega for his help for the artwork, and C. Wendling for her efficiency over a broad range of 'technical' problems.

References

Atreya, S. K., J. H. Waite, Jr., T. M. Donahue, A. F. Nagy, and J. C. McConnell, Theory, measurements, and models of the upper atmosphere and ionosphere of Saturn, in *Saturn*, edited by T. Gehrels and M. S. Matthews, p. 239, Univ. of Arizona Press, Tucson, 1984.

Bahnsen, A., B. M. Pedersen, M. Jespersen, E. Ungstrup, L. Eliasson, J. S. Murphree, R. D. Elphinstone, L. Blomberg, G. Holmgren, and L. J. Zanetti, Viking observations at the source region of Auroral Kilometric Radiation, *J. Geophys. Res.*, **94**, 6643, 1989.

Baumback, M. M., and W. Calvert, The minimum bandwidth of auroral kilometric radiation, *Geophys. Res. Lett.*, **14**, 119, 1987.

Benson, R. F., and W. Calvert, ISIS–1 observations at the source of auroral kilometric radiation, *Geophys. Res. Lett.*, **6**, 479, 1979.

Benson, R. F., and J. Fainberg, Maximum power flux of Auroral Kilometric Radiation, *J. Geophys. Res.*, **96**, 13749, 1991.

Boischot, A., Comparative Study of the 'Radio-Planets', in *Planetary Radio Emissions II*, edited by H. O. Rucker, S. J. Bauer and B. M. Pedersen, p. 15, Austrian Academy of Sciences Press, Vienna, 1988.

Bridge, H. S., F. Bagenal, J. W. Belcher, A. J. Lazarus, R. L. McNutt, J. D. Sullivan, P. R. Gazis, R. E. Hartle, K. W. Ogilvie, J. D. Scudder, E. C. Sittler, A. Eviatar, G. L. Siscoe, C. K. Goertz, and V. M. Vasyliunas, Plasma observations near Saturn: Initial results from Voyager 2, *Science*, **215**, 563, 1982.

Calvert, W., The auroral plasma cavity, *Geophys. Res. Lett.*, **8**, 919, 1981.

Calvert, W., A feedback model for the source of the auroral kilometric radiation, *J. Geophys. Res.*, **87**, 8199, 1982.

Calvert, W., DE–1 measurements of AKR wave directions, *Geophys. Res. Lett.*, **12**, 381, 1985.

Calvert, W., Planetary radio lasing, in *Planetary Radio Emissions II*, edited by H. O. Rucker, S. J. Bauer, and B. M. Pedersen, p.407, Austrian Academy of Sciences Press, Vienna, 1988.

Carr, T. D., and S. Gulkis, The auroral kilometric radiation from Uranus and its magnetospheric implications, in *Planetary Radio Emissions II*, edited by H. O. Rucker, S. J. Bauer, and B. M. Pedersen, p.223, Austrian Academy of Sciences Press, Vienna, 1988.

Connerney, J. E. P., L. Davis, Jr., and D. L. Chenette, Magnetic field models, in *Saturn*, edited by T. Gehrels and M. S. Matthews, p.354, Univ. of Arizona Press, Tucson, Arizona, 1984.

de Feraudy, H., B. M. Pedersen, A. Bahnsen, and M. Jespersen, Viking observations of auroral kilometric radiation from the plasmasphere to night auroral oval source regions, *Geophys. Res. Lett.*, **14**, 511, 1987.

de Feraudy, H., A. Bahnsen and M. Jespersen, Observations of nightside and dayside Auroral Kilometric Radiation with Viking, in *Planetary Radio Emissions II*, edited by H. O. Rucker, S. J. Bauer, and B. M. Pedersen, p.41, Austrian Academy of Sciences Press, Vienna, 1988.

Desch, M. D., M. L. Kaiser, A. Lecacheux, Y. Leblanc, M. Aubier, and A. Ortega–Molina, Uranus as a radio source, in *Uranus*, edited by J. T. Bergstralh, E. D. Miner, and M. S. Matthews, p. 894, Univ. of Arizona Press, Tucson, Arizona, 1991.

Divine N., and H. B. Garrett, Charged particle distributions in Jupiter's magnetosphere, *J. Geophys. Res.*, **88**, 6889, 1983.

Dulk, G. A., A. Lecacheux, and Y. Leblanc, The complete polarization state of a storm of millisecond bursts from Jupiter, *Astron. Astrophys.*, **253**, 292, 1992.

Farrell, W. M., M. D. Desch, M. L. Kaiser, and W. Calvert, Evidence of auroral plasma cavities at Uranus and Neptune from radio bursts observations, *J. Geophys. Res.*, **96**, 19049, 1991.

Galopeau, P., P. Zarka, and D. Le Quéau, Theoretical model of Saturn's kilometric radiation spectrum, *J. Geophys. Res.*, **94**, 8739, 1989.

Galopeau, P., A. Ortega–Molina and P. Zarka, Evidence of Saturn's magnetic field anomaly from Saturnian Kilometric Radiation high–frequency limit, *J. Geophys. Res.*, **96**, 14129, 1991.

Genova, F., Les émissions radio 'aurorales' des planètes, *Ann. Phys. Fr.*, **12**, 57, 1987.

Genova, F., B. M. Pedersen, and A. Lecacheux, Dynamic spectra of Saturn kilometric radiation, *J. Geophys. Res.*, **88**, 8985, 1983.

Hilgers, A., The auroral radiating plasma cavities, *Geophys. Res. Lett.*, **19**, 237, 1992.

Hilgers, A., A. Roux, and R. Lundin, Characteristics of AKR sources: A statistical description, *Geophys. Res. Lett.*, **18**, 1493, 1991.

Huff, R. L., W. Calvert, J. D. Craven, L. A. Frank, and D. A. Gurnett, Mapping of auroral kilometric radiation sources to the aurora, *J. Geophys. Res.*, **93**, 11445, 1988.

Kaiser, M. L., M. D. Desch, and A. Lecacheux, Saturn kilometric radiation: Statistical properties and beam geometry, *Nature*, **292**, 731, 1981.

Kaiser, M. L., and M. D. Desch, Saturnian kilometric radiation: Source locations, *J. Geophys. Res.*, **87**, 4555, 1982.

Kaiser, M. L., M. D. Desch, W. S. Kurth, A. Lecacheux, F. Genova, B. M. Pedersen, and D. R. Evans, Saturn as a radio source, in *Saturn*, edited by T. Gehrels and M. S. Matthews, p. 378, Univ. of Arizona Press, Tucson, 1984.

Kaiser, M. L., M. D. Desch, and J. E. P. Connerney, Radio emission from the magnetic equator of Uranus, *J. Geophys. Res.*, **94**, 2399, 1989.

Kurth, W. S., D. D. Barbosa, D. A. Gurnett, and F. L. Scarf, Electrostatic waves in the magnetosphere of Uranus, *J. Geophys. Res.*, **92**, 15125, 1987.

Lazarus, A. J., and H. R. L. McNutt, Jr., Low energy plasma ion observations in Saturn's magnetosphere, *J. Geophys. Res.*, **88**, 8831, 1983.

Leblanc, Y., M. G. Aubier, C. Rosolen, F. Genova, and J. de la Noë, The Jovian S–bursts. II. Frequency drift measurements at different frequencies throughout several storms, *Astron. Astrophys.*, **86**, 349, 1980.

Lecacheux A., and F. Genova, Source location of Saturn kilometric radio emission, *J. Geophys. Res.*, **88**, 8993, 1983.

Lecacheux, A., Polarization Aspects from Planetary Radio Emissions, in *Planetary Radio Emissions II*, edited by H. O. Rucker, S. J. Bauer, and B. M. Pedersen, p. 311, Austrian Academy of Sciences Press, Vienna, 1988.

Lecacheux, A., A. Boischot, M. Y. Boudjada, and G. A. Dulk, Spectra and complete polarization state of two Io–related radio storms from Jupiter, *Astron. Astrophys.*, **251**, 339, 1991.

Le Quéau, D., Planetary radio emissions from high magnetic latitudes: the 'Cyclotron Maser' theory, in *Planetary Radio Emissions II*, edited by H. O. Rucker, S. J. Bauer, and B. M. Pedersen, p. 381, Austrian Academy of Sciences Press, Vienna, 1988.

Le Quéau, D., R. Pellat, and A. Roux, Direct generation of the auroral kilometric radiation by the maser synchrotron instability: An analytical approach, *Phys. Fluids*, **27**, 247, 1984.

Le Quéau, D., R. Pellat, and A. Roux, The maser synchrotron instability in an inhomogeneous medium: Application to the generation of the auroral kilometric radiation, *Ann. Geophys.*, **3**, 273, 1985.

Le Quéau, D., and P. Louarn, Analytical study of the relativistic dispersion : Application to the generation of AKR, *J. Geophys. Res.*, **94**, 2605, 1989.

Louarn, P., A. Roux, H. de Feraudy, D. Le Quéau, M. André, and L. Matson, Trapped electrons as a free energy source for the Auroral Kilometric Radiation, *J. Geophys. Res.*, **95**, 5983, 1990.

McNutt, R. L., R. S. Selesnick, and J. D. Richardson, Low–energy plasma observations in the magnetosphere of Uranus, *J. Geophys. Res.*, **92**, 4399, 1987.

Melrose, D. B., R. G. Hewitt, and G. A. Dulk, Electron cyclotron Maser emission: Relative growth and damping rates for different modes and harmonics, *J. Geophys. Res.*, **89**, 897, 1984.

Melrose, D. B., and G. A. Dulk, On the elliptical polarization of Jupiter's decametric radio emission, *Astron. Astrophys.*, **249**, 250, 1991.

Mizera, P. F., and J. F. Fennel, Signature of electric fields from high and low altitude particle distribution, *Geophys. Res. Lett.*, **4**, 311, 1977.

Ness, N. F., The magnetic environment of the known radio planets, in *Planetary Radio Emissions II*, edited by H. O. Rucker, S. J. Bauer, and B. M. Pedersen, p. 3, Austrian Academy of Sciences Press, Vienna, 1988.

Ness, N. F., M. H. Acuña, K. W. Behannon, L. F. Burlaga, J. E. P. Connerney, R. P. Lepping, and F. M. Neubauer, Magnetic fields at Uranus, *Science*, **233**, 85, 1986.

Pedersen, B. M., A. Lecacheux, P. Zarka, M. G. Aubier, M. L. Kaiser, and M. D. Desch, Phenomenology of Neptune's radio emissions observed by the Voyager planetary radio astronomy experiment, *J. Geophys. Res.*, in press, 1992.

Perraut, S., H. de Feraudy, A. Roux, P. M. E. Decreau, J. Paris, and L. Matson, Density measurements in key regions of the Earth's magnetosphere: Cusp and auroral region, *J. Geophys. Res.*, **95**, 5997, 1990.

Persoon, A. M., D. A. Gurnett, W. K. Peterson, J. H. Waite Jr, J. L. Burch, and J. L. Green, Electron density depletions in the nightside auroral zone, *J. Geophys. Res.*, **93**, 1871, 1988.

Pritchett, P. L., Relativistic dispersion, the cyclotron maser instability, and auroral kilometric radiation, *J. Geophys. Res.*, **89**, 8957, 1984.

Richardson, J. D., and E. C. Sittler Jr., A plasma density model for Saturn based on Voyager observations, *J. Geophys. Res.*, **95**, 12019, 1990.

Sandel, B. R., D. E. Shemansky, A. L. Broadfoot, J. B. Holberg, G. R. Smith, J. C. McConnel, D. F. Strobel, S. K. Atreya, T. M. Donahue, H. W. Moos, D. M. Hunten, R. B. Pomphrey, and S. Linick, Extreme ultraviolet observations from the Voyager 2 encounter with Saturn, *Science*, **215**, 548, 1982.

Sawyer, C. B., J. W. Warwick, and J. H. Romig, Smooth radio emission and a new emission at Neptune, *Geophys. Res. Lett.*, **17**, 1645, 1990.

Stone, R. G., J. L. Bougeret, J. Caldwell, P. Canu, Y. de Conchy, N. Cornilleau–Wehrlin, M. D. Desch, J. Fainberg, K. Goetz, M. L. Goldstein, C. C. Harvey, S. Hoang, R.

Howard, M. L. Kaiser, P. J. Kellog, B. Klein, R. Knoll, A. Lecacheux, D. Lengyel–Frey, R. J. MacDowall, R. Manning, C. A. Meetre, A. Meyer, N. Monge, S. Monson, G. Nicol, M. J. Reiner, J. L. Steinberg, E. Torres, C. de Villedary, F. Wouters, and P. Zarka, The unified radio and plasma wave investigation, *Astron. Astrophys. Suppl. Ser.*, **92**, 291, 1992.

Temerin, M., Electron density and whistler mode propagation characteristics at 7000 km altitude in the auroral zone and polar cap, *J. Geophys. Res.*, **89**, 3945, 1984.

Temerin, M., C. A. Catell, R. Lysak, M. Hudson, R. B. Torbert, F. S. Mozer, R. D. Sharp, and P. M. Kintner, The small–scale structure of electrostatic shocks, *J. Geophys. Res.*, **86**, 11278, 1981.

Tyler, G. L., V. R. Eshleman, J. D. Anderson, G. S. Levy, G. F. Lindal, G. E. Wood, and T. A. Croft, Radio science with Voyager 2 at Saturn: Atmosphere and ionosphere and the masses of Mimas, Tethys, and Iapetus, *Science*, **215**, 553, 1982.

Warwick, J. W., J. B. Pearce, R. G. Peltzer, and A. C. Riddle, Planetary Radio Astronomy experiment for Voyager missions, *Space Sci. Rev.*, **21**, 309, 1977.

Warwick, J. W., D. R. Evans, G. R. Peltzer, R. G. Peltzer, J. H. Romig, C. B. Sawyer, A. C. Riddle, A. E. Schweitzer, M. D. Desch, M. L. Kaiser, W. M. Farrell, T. D. Carr, I. de Pater, D. H. Staelin, S. Gulkis, R. L. Poynter, A. Boischot, F. Genova, Y. Leblanc, A. Lecacheux, B. M. Pedersen, P. Zarka, Voyager Planetary Radio Astronomy at Neptune, *Science*, **246**, 1498, 1989.

Wu, C. S., Kinetic cyclotron and synchrotron maser instabilities: Radio emission processes by direct amplification of radiation, *Space Sci. Rev.*, **41**, 215, 1985.

Wu, C. S., and L. C. Lee, A theory of the terrestrial kilometric radiation, *Astrophys. J.*, **230**, 621, 1979.

Zaitsev, V. V., E. Y. Zlotnik, and V. E. Shaposhnikov, The origin of S–bursts in Jupiter's decametric radio spectra, *Astron. Astrophys.*, **169**, 345, 1986.

Zarka, P., Beaming of Planetary Radio Emissions, in *Planetary Radio Emissions II*, edited by H. O. Rucker, S. J. Bauer, and B. M. Pedersen, p. 327, Austrian Academy of Sciences Press, Vienna, 1988.

Zarka, P., The Auroral Radio Emissions from Planetary Magnetospheres, what do we know, what don't we know, what do we learn from them ?, *Adv. Space Res.*, **12**, (8)99, 1992.

Zarka, P., D. Le Quéau, and F. Genova, The maser synchrotron instability in an inhomogeneous medium: Determination of the spectral intensity of auroral kilometric radiation, *J. Geophys. Res.*, **91**, 13542, 1986.

Zarka, P., and A. Lecacheux, Beaming of Uranian nightside kilometric radio emission and inferred source location, *J. Geophys. Res.*, **92**, 15177, 1987.

The field of remote sensing began with aerial pho-tography, using visible light from the sun as the energy source. But visible light makes up only a small part of the electromagnetic spectrum, a con-tinuum that ranges from high energy, short wavelength gamma rays, to lower energy, long wave-length radio waves.Â The spectral resolution of a remote sensing system can be described as its ability to distinguish different parts of the range of measured wavelengths. In essence, this amounts to the number of wavelength intervals (â€œbandsâ€) that are measured, and how narrow each interval is. An â€œimageâ€ produced by a sensor system can consist of one very broad wavelength band, a few broad bands, or many narrow wavelength bands. Radar remote sensing. Use Super Dual Auroral Network (SuperDARN) of HF radars. to identify separatrixand. to measure E x B velocity.Â Distributions of areas and durations of auroral bright spots are power law (scale-free) from kinetic to system scales [Uritsky et al., JGR, 2002; Borelov and Uritsky, private communication]. Could this be associated with multi-scale reconnection in the magnetotail? Self-organisation of reconnection to critical state (SOC) [e.g., Chang, Phys.Â Plasma in the solar system: science and missions Stas Barabash -Plasma in the solar system: science and missions stas barabash swedish institute of space physics (irf) kiruna, sweden. swedish institute of space physics. established 1957 a.